

By expressing the sines as exponentials, and comparing the resulting equation with (I.4), we have

$$A_{JM_p} = [2\pi(2J+1)]^{1/2} D_{M\Omega}^J(\hat{k}) \quad (\text{I.7})$$

Appendix II

From eq 42, the angular distribution for an initial state J is

$$P^J(\theta) = \frac{\cos^2 \theta}{2} \sum_{l,M} \frac{(-1)^{M-\Omega}}{\Gamma_M} \langle JJM - M | l, 0 \rangle \langle JJ\Omega - \Omega | l, 0 \rangle P_l(\cos \theta) \quad (\text{II.1})$$

At $\theta = 0$, $P_l(\cos \theta) = 1$, we obtain

$$P^J(0) = \frac{1}{2} \sum_M \frac{(-1)^{M-\Omega}}{\Gamma_M} \left[\sum_l \langle JJM - M | l, 0 \rangle \langle JJ\Omega - \Omega | l, 0 \rangle \right] = \frac{1}{2} \sum_M \frac{(-1)^{M-\Omega}}{\Gamma_M} \delta_{M,\Omega} = \frac{1}{2\Gamma_{1/2}} \quad (\text{II.2})$$

Now for incident Z polarization, from (36b) one readily obtains^{10,11}

$$\Gamma_M = \frac{1}{2} \left(1 - \frac{M^2}{J(J+1)} \right) \quad (\text{II.3})$$

so that finally

$$P^J(0) = \frac{J(J+1)}{J(J+1) - 1/4} \quad (\text{II.4})$$

Appendix III

The branching ratios shown in Table II are easily explained by using a simple model. We take into consideration the fact that the dominant coupling are given by $\Delta J = \pm 1$ and consider a system where three bound states $|J\rangle$,

$|J-2\rangle$, $|J+2\rangle$ are mixed through transitions via continuum states, as shown in Figure 4.

We assume $E_{J+2} - E_J = E_J - E_{J-2} = \Delta$ and that the couplings are independent of J . By writing $y = \int dE_c (V_{ic} V_{ci}) / (E^+ - E_c)$, we can express $H_0 + QtQ$ in a matrix form as

$$\begin{bmatrix} E_J - \Delta + 2y & y & 0 \\ y & E_J + 2y & y \\ 0 & y & E_J + \Delta + 2y \end{bmatrix} \quad (\text{III.1})$$

which can be diagonalized to obtain the dressed states $|\tilde{J}\rangle$, $|J-2\rangle$, $|J+2\rangle$. One readily obtains the following expression for the J level

$$|\tilde{J}\rangle = \frac{1}{(\Delta^2 + 2y^2)^{1/2}} \Delta |J\rangle + y[|J-2\rangle - |J+2\rangle] \quad (\text{III.2})$$

From eq 34, one can see that the transition amplitudes evaluated at $E_b = E_J$ are proportional to

$$T_{J'} \propto \langle J' | V | \tilde{J} \rangle = \frac{1}{(\Delta^2 + 2y^2)^{1/2}} [\Delta V_{JJ} + yV_{JJ-2} - yV_{JJ+2}] \quad (\text{III.3})$$

We can use this last equation with the selection rules $J' = J \pm 1$

$$\left| \frac{T_{J-1}}{T_{J+1}} \right| = \left| \frac{\Delta + y}{\Delta - y} \right|^2 \quad (\text{III.4})$$

Thus for $y > 0$, $\Delta J = -1$ photodissociation is enhanced. Since y is essentially an energy shift, it is usually positive for levels above the crossing point (Figure 1^{16,28}).

Registry No. Ar₂⁺, 17596-58-6.

(28) A. D. Bandrauk and J. P. Laplante, *J. Chem. Phys.*, **65**, 2592 (1976).

Energy Partitioning to Product Translation in the Infrared Multiphoton Dissociation of Diethyl Ether

L. J. Butler, R. J. Buss,[†] R. J. Brudzynski, and Y. T. Lee*

Materials and Molecular Research Division, Lawrence Berkeley Laboratory and Department of Chemistry, University of California, Berkeley, California 94720 (Received: June 10, 1983)

The infrared multiphoton decomposition of diethyl ether (DEE) has been investigated by the cross laser-molecular beam technique. The center-of-mass product translational energy distributions ($P(E')$) were measured for the two dissociation channels: (1) DEE \rightarrow C₂H₅O + C₂H₅ and (2) DEE \rightarrow C₂H₅OH + C₂H₄. The shape of the $P(E')$ measured for radical channel 1 is in agreement with the predictions of statistical unimolecular rate theory. The translational energy released in concerted reaction 2 peaks at 24 kcal/mol; this exceedingly high translational energy release with a relatively narrow distribution results from the recoil of the products from each other down the exit barrier. Applying statistical unimolecular rate theory, we estimate the average energy levels from which DEE dissociates to products using the measured $P(E')$ for radical channel 1.

I. Introduction

Previous molecular beam investigations of unimolecular reaction dynamics have shown that potential energy barriers in the exit channel beyond the endoergicity have a large effect on the asymptotic product translational energy

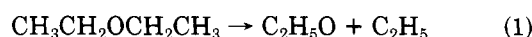
distributions. For almost all of the simple fission reactions studied, in which a single bond is broken without an exit barrier and no new bonds are formed, the products have statistical translational energy distributions.¹ However, for all the complex fission reactions studied, in which

[†] Present address: Sandia National Laboratory, Division 1811, Albuquerque, NM 87185.

(1) Aa. S. Sudbo, P. A. Schulz, E. R. Grant, Y. R. Shen, and Y. T. Lee, *J. Chem. Phys.*, **70**, 912 (1979).

bonds are broken and formed simultaneously, the translational energy distributions of the products reflect their recoil from each other down the substantial potential energy barrier in the exit channel.²⁻⁴ Huisken et al.² studied the infrared multiphoton dissociation (IRMPD) of ethyl vinyl ether (EVE) in a crossed laser-molecular beam apparatus. They observed competition between two dissociation channels: (1) $\text{EVE} \rightarrow \text{CH}_3\text{CHO} + \text{C}_2\text{H}_4$ and (2) $\text{EVE} \rightarrow \text{CH}_2\text{CHO} + \text{C}_2\text{H}_5$ and found that approximately 70% of the 38 kcal/mol exit barrier for reaction 1 was released into product translational energy. Such a high translational energy release, ~ 30 kcal/mol, in the unimolecular dissociation of a polyatomic molecule in the ground electronic state was previously unsuspected. Several other similar experiments, which measured the product translational energy distributions for reactions involving three- and four-center HCl elimination from halogenated hydrocarbons³ and a three-center Cl_2 elimination from CF_2Cl_2 ,⁴ are reviewed in the paper of Huisken et al. In the four-center elimination of hydrogen halides, a large fraction of the exit barrier appears as vibrational excitation of the products; the average translational energy release does not usually exceed 10 kcal/mol. Also reviewed there are some examples of infrared⁵ and laser-induced fluorescence⁶ techniques used in bulk experiments to measure the internal energy distributions of products from complex fission reactions.

Two groups have independently studied the thermal decomposition of diethyl ether (DEE) and derived preexponential factors and activation energies for the Arrhenius expression for the rate constants of the primary dissociation processes. Laidler and McKenney⁷ and István and Péter⁸ both report two competing primary channels, a simple C-O bond fission reaction with little or no exit barrier



and a molecular elimination reaction with a large exit barrier



The Arrhenius parameters for the four-centered elimination (2) were reported to be $\log A = 18.0$ and $E_a = 84$ kcal/mol by Laidler and McKenney, and $\log A = 13.9$ and $E_a = 66.0$ by István and Péter. The A factor and activation energy for the radical channel were reported to be 14.0 and 78 kcal/mol respectively by Laidler and McKenney and 14.3 and 77.5 by István and Péter. Benson and O'Neal⁹ point out that the Laidler and McKenney A factors are not reliable as (2) should have a larger, more positive entropy of activation than (1) so it is expected that the A factor of (2) is larger than that of (1). They also point out that a fairly reliable estimate for the parameters of the radical reaction 2 can be made from the thermodynamics by assuming a recombination rate of $k_{\text{rec}} = 10^{9.7 \pm 1.0} \text{ L}/(\text{mol s})$, from which they obtain $\log A = 16.3$ and $E_a = 81.8$. The other energetically allowed decomposition channels are shown in Figure 1 along with these two channels. The

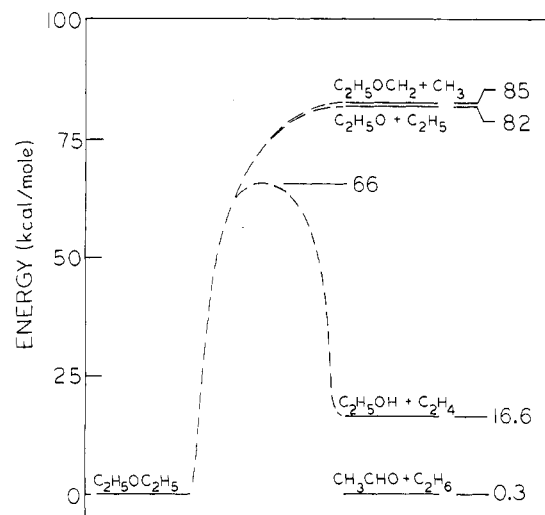


Figure 1. The low-energy dissociation channels of $\text{C}_2\text{H}_5\text{OC}_2\text{H}_5$. ΔH°_{300} values were calculated from values tabulated in Rosenstock et al. (*J. Phys. Chem. Ref. Data*, **6**, Suppl. 1 (1977)) for the ethanol and acetaldehyde channels and estimated to be 85 kcal/mol for the $\text{C}_2\text{H}_5\text{OCH}_2$ channel by using group additivity rules (S. W. Benson, "Thermochemical Kinetics", Wiley-Interscience, New York, 1976) and the heat of formation of CH_3OCH_2 . The energetics of the $\text{C}_2\text{H}_5\text{O} + \text{C}_2\text{H}_5$ radical channel are those of ref 9. The barrier in the ethanol channel, 66 kcal/mol from the reactant, was reported in ref 8.

activation energies shown are those estimated by Benson and O'Neal for radical channel 1 and reported by István and Péter for molecular elimination reaction 2.

Thus this system allowed the molecular beam study of two competing dissociation channels, one a concerted reaction with a constrained transition state resulting in a large exit barrier and the other a simple bond fission reaction with a large activation energy but no significant exit barrier. We wished to confirm the identification of these two channels, to investigate the possibility of the occurrence of the other two energetically allowed channels shown in Figure 1 and to determine the effect of the large exit channel barrier for reaction 1 on the product translational energy distribution. As will be seen, the velocity distributions of the radical channel products allowed us to determine limits on the energy levels from which the molecules dissociated, thus providing an estimate on the average number of photons absorbed in our IRMPD experiment.

II. Experiment

Time-of-flight (TOF) distributions of the photofragments were measured in a molecular beam apparatus described in detail elsewhere.¹⁰ The molecular beam was formed by bubbling helium through diethyl ether (DEE) (Mallinckrodt AR grade) maintained at 0 °C and expanding the mixture through a 0.13-mm-diameter stainless-steel nozzle at a total stagnation pressure of 400 torr ($\sim 50\%$ DEE/ 50% He). The nozzle was heated to 300 °C to eliminate the formation of molecular clusters during the supersonic expansion. The velocity distribution of the DEE beam was determined by TOF measurements to have a peak velocity of 1120 m/s and a full width at half-maximum of 30%. The beam was collimated by a skimmer and, after passing through two pressure-reducing differential-pumping chambers, it was crossed with the laser beam. The molecular beam was defined to an angular divergence of $\sim 1.6^\circ$.

(2) F. Huisken, D. Krajnovich, Z. Zhang, Y. R. Shen, and Y. T. Lee, *J. Phys. Chem.*, **78**, 3806 (1983).

(3) Aa. S. Sudbo, P. A. Schulz, Y. R. Shen, and Y. T. Lee, *J. Chem. Phys.*, **69**, 2312 (1978).

(4) D. Krajnovich, F. Huisken, Z. Zhang, Y. R. Shen, and Y. T. Lee, *J. Chem. Phys.*, **77**, 5977 (1982).

(5) C. R. Quick, Jr., and C. Wittig, *J. Chem. Phys.*, **72**, 1694 (1980).

(6) D. S. King and J. C. Stephenson, *Chem. Phys. Lett.*, **51**, 48 (1977);

J. C. Stephenson and D. S. King, *J. Chem. Phys.*, **69**, 2485 (1978).

(7) K. J. Laidler and D. J. McKenney, *Proc. R. Soc. London, Ser. A*, **278**, 517 (1964).

(8) S. István and H. Péter, *Mag. Kem. Foly.*, **81**, 120 (1975).

(9) S. W. Benson and H. E. O'Neal, *Natl. Stand. Ref. Data Ser., Natl. Bur. Stand.*, **No. 21** (1970).

(10) Y. T. Lee, J. D. McDonald, P. R. LeBreton, and D. R. Herschbach, *Rev. Sci. Instrum.*, **40**, 1402 (1969).

The infrared photons were produced by a Gentec DD-250 CO₂ TEA laser tuned to the P(24) line in the 001–020 vibrational band at 1043.16 cm⁻¹. The TT conformer of DEE has an absorption band at 1047 cm⁻¹ and the less stable (by 1.1 kcal/mol) TG conformer absorbs at 1021 and 1067 cm⁻¹.¹¹ A photon drag detector was used to measure the temporal output of the laser pulse; the intensity is strongest near the beginning of the pulse, which has a 300-ns fwhm and a long tail extending to 600 ns with an average intensity of ~40% of the peak. The laser was run at a 50-Hz repetition rate. For all the TOF data, but the *m/e* 26 TOF, the total energy fluence crossing the molecular beam in the interaction region is estimated to be ~2.4 J/cm². The *m/e* 26 TOF was taken at an energy fluence of ~1.8 J/cm². The laser light was unpolarized and was focused onto the molecular beam with a 25-in. focal length spherical zinc selenide lens. For the total signal dependence on laser fluence, the lens position was kept fixed and the fluence was adjusted from 0.5 to 5.5 J/cm² by attenuating the laser beam by passing it through a gas cell filled with C₂H₂ at pressures from 0 to 360 torr.

The dissociation products were detected in the plane of the laser and molecular beam by a rotatable ultrahigh vacuum mass spectrometer consisting of an electron bombardment ionizer, quadrupole mass filter, and particle counter. The emission current in the ionizer was 10 mA with a 240-eV electron energy. The flight path between the beam crossing point and the ionizer was 20.7 cm. TOF distributions were measured in the usual way.¹²

Signal was observed when the quadrupole mass spectrometer was set to pass the following mass-to-charge ratios: *m/e* 14, 15, 26, 27, 28, 29, 30, 31, and 44; after very long counting time a very small signal was detected at *m/e* 57. These masses correspond to CH₂⁺, CH₃⁺, C₂H₂⁺, C₂H₃⁺, (CO⁺, C₂H₄⁺), (C₂H₅⁺, CHO⁺), (CH₂O⁺, CHOH⁺), (CH₂OH⁺, CH₃O⁺), and C₂H₄O⁺ and to C₂H₅OCH⁺. No measurable signal was detected at *m/e* 46, 58, or 59 corresponding to C₂H₅OH⁺, C₂H₄OCH₂⁺, and C₂H₅OCH₂⁺ or their isomers after signal averaging for 300 000 laser shots for each. The data taken at *m/e* 45 (C₂H₅O⁺) were discarded when it was found that the *m/e* 44 data taken that day showed evidence of poor mass tuning of the quadrupole. Typical signal levels at a detection angle of 10° from the molecular beam and a photon fluence of ~2.4 J/cm² ranged from 0.14 to 0.82 counts/laser pulse for all but *m/e* 57, at which the signal level was 0.003 counts/laser pulse. A good signal-to-noise ratio was obtained for all masses but 14, 15, and 57.

Results and Analysis

A. Identification of the Molecular Elimination Channel. The *m/e* 31 (CH₂OH⁺, CH₃O⁺) TOF measured at an angle of 10° to the molecular beam is shown in Figure 2. Let us first focus our attention on the faster peak in this spectrum. This sharp feature, which corresponds to a narrow energy distribution at a relatively high average translational energy, can only contain contributions from the heavier molecule of each pair of products shown in Figure 1. It is easily calculated, from momentum and energy conservation, that about 24 kcal/mol of the total available energy would have had to be released as translational energy of the products for the acetaldehyde, ethanol, or ethoxy radical product to arrive at the detector at times corresponding to the peak of the fast distribution in the *m/e* 31 TOF. The total product translational energy

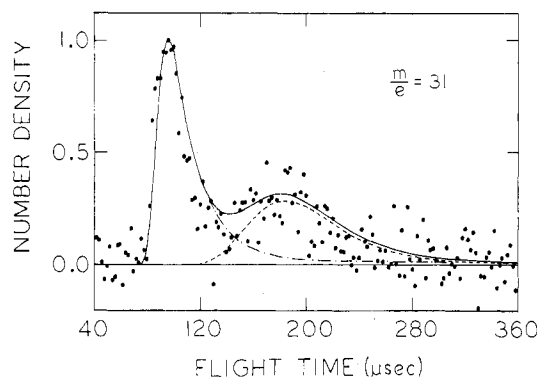


Figure 2. TOF distribution of *m/e* 31 (CH₂OH⁺, CH₃O⁺) at 10° from the molecular beam: (●) experimental points; (—) best fit obtained by adding the individual contributions of C₂H₅OH (---) and C₂H₅O (···). The C₂H₅OH contribution was calculated from the *P(E')* in Figure 11. The C₂H₅O contribution was calculated from the *P(E')* in Figure 9. The relative intensities were varied to obtain the best fit and an isotropic center-of-mass angular distribution was used. Photon energy fluence = 2.4 J/cm². Note that the time scale in this and all subsequent TOF spectra include the transit time of the ion through the mass spectrometer. (For our operating conditions, the ion transit time in μs is 2.0*M*^{1/2} where *M* is the detected ion mass in amu.) To convert to laboratory velocity, one must correct the displayed flight times for the ion transit time and divide it into the flight path, 20.7 cm. For an example of this transformation, see Figures 3a and 3b.

would have to be as much as 115 kcal/mol at the peak of the distribution if the C₂H₅OCH₂ product were responsible for the fast peak in the *m/e* 31 TOF spectrum. Thus, it is very clear that the fast velocity product in the mass 31 TOF must be due to one of the two energetically allowed molecular elimination reactions as only these two channels have enough energy available through the conversion of the exit potential energy barrier to give the observed product translational energies. The radical channels from simple bond rupture are not expected to have such a high average translational energy release with such a narrow energy distribution, even if an excessively large number of photons are absorbed before dissociation.

Identification of the molecular elimination channel would be easy if we had observed the same fast product velocity distribution at *m/e* 46, (C₂H₅OH⁺), but the fast product was not observed at this mass or at *m/e* 44 (CH₃CHO⁺, CH₂CHOH⁺). This is understandable because the energies required to dissociate C₂H₅OH⁺ or CH₃CHO⁺ to their smaller ion fragments are known to be small, ~15 kcal/mol, and the ionization of highly vibrationally excited C₂H₅OH or CH₃CHO products is not expected to yield the parent ion in electron bombardment ionization. By careful examination of the masses at which daughter ions of the heavy product appear and of the masses at which daughter ions of the lighter partner (C₂H₄ for the ethanol product or C₂H₆ for the acetaldehyde product) appear, one can be reasonably certain that DEE dissociates to form ethanol and ethylene but not acetaldehyde and ethane. First, *m/e* 31 is the major ion mass fragment of ethanol.¹³ Second, no signal from acetaldehyde was detected at *m/e* 31 in a previous IRMPD experiment on the same apparatus in which acetaldehyde was a product;² an H atom migration must occur to get signal from acetaldehyde at *m/e* 31 (CH₂OH⁺). Third and perhaps most important, the lighter fragment of the molecular elimination channel does not appear in the *m/e* 30 or 29 TOF spectra (see Figures 3 and 4) but it does appear in the *m/e* 28 spectra. If the C₂H₆ product were being formed one would expect it to give *m/e*

(11) H. Wieser, W. G. Laidlaw, P. J. Krueger, and H. Fuhrer, *Spectrochim. Acta, Part A*, **24**, 1055 (1967).

(12) See, for example, ref 3.

(13) E. Stenhagen, S. Abrahamsson, and F. W. McLafferty, Ed., "Atlas of Mass Spectral Data", Wiley, New York, 1969.

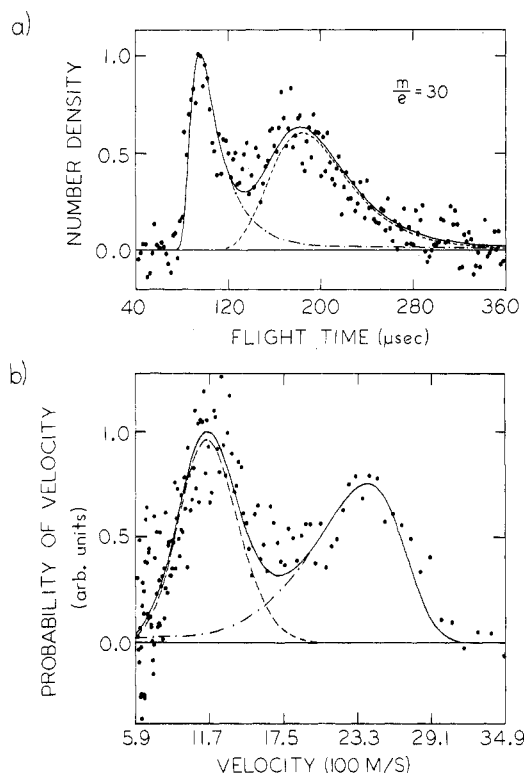


Figure 3. (a) TOF distribution of m/e 30 (CHOH^+ , CH_2O^+) at 10° from the molecular beam: (●) experimental points; (—) best fit obtained by adding the individual contributions of $\text{C}_2\text{H}_5\text{OH}$ (---) and $\text{C}_2\text{H}_5\text{O}$ (---). The individual contributions were calculated as in Figure 2. Photon energy fluence = 2.4 J/cm^2 . (b) Laboratory velocity flux distribution of m/e 30 derived from the TOF distribution between 360 and 70 μs . The center-of-mass velocity may be approximately obtained by subtracting $1120 \text{ m/s} \times \cos 10^\circ$ from the laboratory velocity.

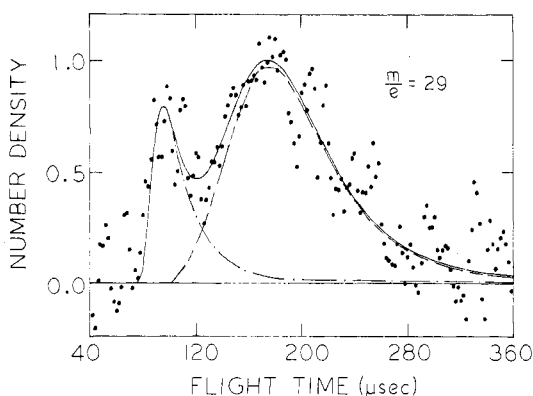


Figure 4. TOF distribution of m/e 29 (CHO^+ , C_2H_5^+) at 10° from the molecular beam. Data are shown with a five-point polynomial smooth: (●) experimental points; (—) best fit obtained by adding the individual contributions of $\text{C}_2\text{H}_5\text{OH}$ (---) and C_2H_5 (---). The $\text{C}_2\text{H}_5\text{OH}$ contribution was calculated as in Figure 2. The C_2H_5 contribution was calculated from the $P(E')$ shown in Figure 9 which is derived from the $\text{C}_2\text{H}_5\text{O}$ TOF distribution (Figure 6). Photon energy fluence = 2.4 J/cm^2 .

30 or 29, yet there is no additional broadening of the fast peak in the m/e 30 or 29 TOF which is expected from the lighter fragment. The lighter, faster product is not detected until the m/e is tuned to 28 (C_2H_4^+), as would be expected if DEE dissociates to give ethanol and ethylene. The TOF of m/e 28 is shown in Figure 5.

B. Identification of the Radical Channel. The TOF spectra of m/e 44 ($\text{C}_2\text{H}_4\text{O}^+$) at 10° from the molecular beam is shown in Figure 6. The fast partner to this velocity distribution appears in the TOF spectra taken at masses m/e 29, 28, 27 (Figure 7), 26 (Figure 8), 15, and 14. Thus the radical channel, reaction 1, which forms $\text{C}_2\text{H}_5\text{O}$

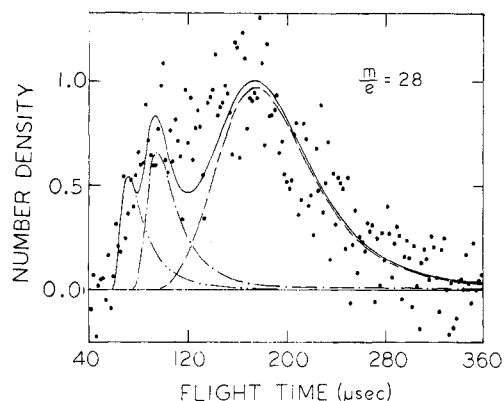


Figure 5. TOF distribution of m/e 28 (CO^+ , C_2H_4^+) at 10° from the molecular beam: (●) experimental points; (—) best fit obtained by adding the individual contributions of C_2H_4 (---), $\text{C}_2\text{H}_5\text{OH}$ (---), and C_2H_5 (---). The shape of each individual TOF distribution is fixed by the $P(E')$ that fit the m/e 44 and 31 TOF's (Figures 6 and 2). The relative intensity of each contribution was varied to obtain best fit.

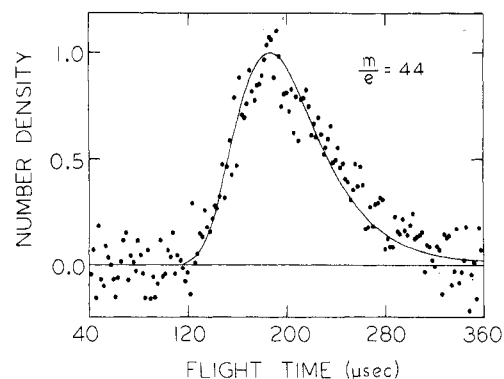


Figure 6. TOF distribution of $m/e = 44$ ($\text{C}_2\text{H}_4\text{O}^+$) at 10° from the molecular beam: (●) experimental points; (—) fit calculated from the $P(E')$ in Figure 9 and an isotropic center-of-mass angular distribution. Photon energy fluence = 2.4 J/cm^2 .

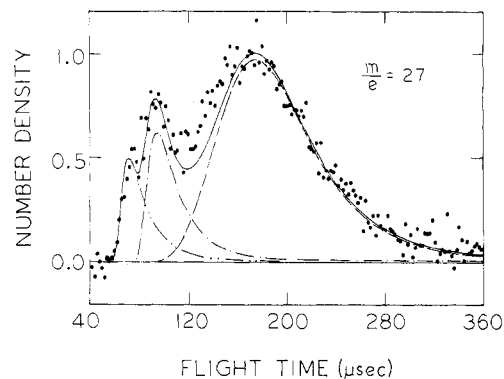


Figure 7. TOF distribution of m/e 27 (C_2H_3^+) at 10° from the molecular beam: (●) experimental points; (—) best fit obtained by adding the individual contributions of C_2H_4 , $\text{C}_2\text{H}_5\text{OH}$, and C_2H_5 as in Figure 5. Photon energy fluence = 2.4 J/cm^2 .

+ C_2H_5 must be occurring since the CH_3 product in the other radical channel cannot give any contribution at the higher of the masses. The extremely small signal at m/e 57 (0.003 counts/laser pulse) suggests that a small fraction of the DEE may dissociate by breaking a C-C bond:



However, this small signal may underestimate the extent of dissociation via reaction 3 as $\text{C}_2\text{H}_5\text{OCH}_2$ may not fragment to give m/e 57, 58, or 59. The contribution of $\text{C}_2\text{H}_5\text{OCH}_2$ and CH_3 to smaller ion masses would largely be obscured by the overlapping TOF spectra of the other

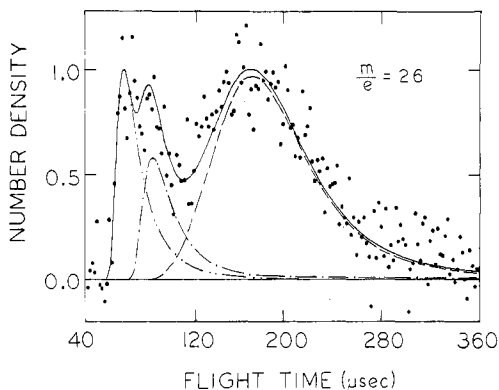


Figure 8. TOF distribution of m/e 26 ($C_2H_2^+$) at 10^9 from the molecular beam: (●) experimental points; (—) best fit obtained by adding the individual contributions of C_2H_4 (····), C_2H_5OH (-·-·-), and C_2H_5 (- - -). The shape of each individual TOF distribution is fixed by the $P(E')$ that fit the m/e 44 and 31 TOF's (Figures 6 and 2). The relative intensity of each contribution was varied to obtain best fit. Photon energy fluence = 1.8 J/cm^2 .

dissociation products. The dissociation of DEE into two channels with vastly different translational energy distributions can also be seen easily in Figure 8 as this TOF has contributions from both of the molecular elimination products and the lighter radical product. The momentum-matched heavier radical product and the heavier molecular product can be seen in Figures 2 and 3 without contributions from the overlapping lighter products.

C. Product Translational Energy Distributions: 1. $C_2H_5OC_2H_5 \rightarrow C_2H_5O + C_2H_5$. When a molecule dissociates to two fragments, the linear momentum of one fragment is equal in magnitude and opposite in direction to that of the other fragment in the center-of-mass coordinate system, so the measured velocity distribution of one derived from the experimental measurements will completely define the velocity distribution of the other fragment and the total center-of-mass translational energy distribution, $P(E')$, of the dissociation process. The TOF distribution of the C_2H_5O product (Figure 6) was fit by a trial and error forward convolution method using a completely flexible point form for the $P(E')$. The good fit shown in Figure 6 was calculated from the $P(E')$ in Figure 9. We used this $P(E')$ to fit the slow peak in the m/e 26 and 27 TOF spectra (Figures 8 and 7) by varying the relative amounts of C_2H_5O and C_2H_5 product contributing to these TOF distributions. In both cases the best fit was obtained when only the C_2H_5 product's contribution was used.

During the trial and error fitting procedure of the m/e 44 TOF, a daughter ion of the C_2H_5O product, it was immediately found that the better fits were achieved by making the $P(E')$ peak at translational energies near 0 kcal/mol. We then tried to fit the data with a translational energy distribution derived with RRKM theory. In an IRMPD experiment the molecules dissociate from a distribution of levels above the dissociation limit determined by the experimental conditions. Thus the RRKM translational energy distribution used to fit the data should be a sum of the translational energy distributions from single energy levels weighted by the fraction of molecules that dissociate from each level. In order to estimate weighting factors for these levels, we simulated the infrared photon absorption and dissociation process for this system with a simple rate equation model described in detail elsewhere.¹⁴ We calculated the RRKM dissociation rate constants (see Figure 10) from published molecular vibrational frequencies and frequencies of transition states

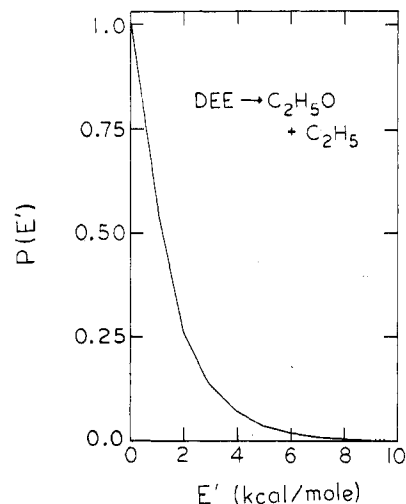


Figure 9. Center-of-mass translational energy distribution for the radical dissociation channel $DEE \rightarrow C_2H_5O + C_2H_5$ derived from the m/e 44 ($C_2H_4O^+$) TOF distribution (Figure 6). This $P(E')$ was used to obtain the calculated fits shown in all other TOF distributions which contained contributions from C_2H_5O or C_2H_5 .

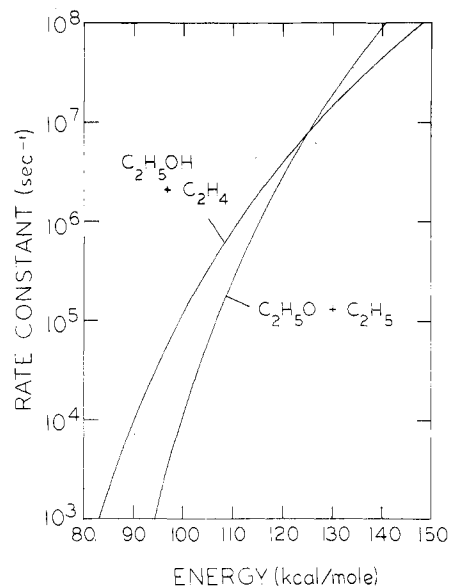


Figure 10. RRKM rate constant curves for DEE decomposition obtained by assuming $E_a = 66 \text{ kcal/mol}$ and $\log A = 13.9$ for the reaction producing $C_2H_5OH + C_2H_4$ and $E_a = 81.8$ and $\log A = 16.3$ for the reaction producing $C_2H_5O + C_2H_5$.

chosen to reproduce the A factor and activation energy estimated by Benson and O'Neal for the radical channel and the reported parameters of István and Péter for the molecular elimination channel (at 800 K). This procedure is known to give reasonable RRKM rate constants as a function of internal energy.¹⁵ The spread of dissociating energy levels was found to be only weakly dependent on the parameters of the model which are not known, most importantly, the change in photon absorption and stimulated emission cross section as a function of internal energy. The simulation suggested a representative form for the relative dissociation yields from a group of neighboring energy levels which we use to calculate the effective RRKM $P(E')$. With each level spaced 2.983 kcal/mol apart, corresponding to the photon energy, the contribution from neighboring energy levels to the RRKM translational energy distribution were weighted by factors of 8, 20, 38, 60,

(14) P. A. Schulz, Ph.D. Thesis, University of California, 1979.

(15) P. J. Robinson and K. A. Holbrook, "Unimolecular Reactions", Wiley, New York, 1972.

73, 80, 73, 60, 38, 20, 8;¹⁶ this dissociating population distribution was used to calculate the RRKM $P(E')$ at several median dissociation energies. The data were then fit by using the resulting $P(E')$ for each mean energy. The model calculation took into account the fact that we could only detect dissociation occurring while the excited molecule was in the viewing region of the detector. It also included the competition between the three competitive processes above the dissociation limits: dissociation to radical products, dissociation to molecular products, and change in energy level due to absorption or stimulated emission of a photon. The unknown parameters in the model, which related to the absorption and stimulated emission of photons, had a large effect on the actual median energy level from which dissociation occurred, but, as will be seen, fitting of the product velocity distribution from the radical channel helped limit the uncertainty in this energy level.

We then attempted to fit the m/e 44 TOF with several different averaged RRKM translational energy distributions. The best fit was achieved with molecules dissociating from 11 energy levels 1.73, 4.71, 7.69, 10.68, 13.66, 16.64, 19.63, 22.61, 25.59, 28.57, and 31.56 kcal/mol above the 81.8-kcal/mol dissociation limit. The translational energy distributions, calculated from RRKM theory, from each of these levels was weighted by the population distribution above and summed to give the $P(E')$ used to fit the data. We will call this the "averaged 16.64-kcal/mol $P(E')$ ". This is the $P(E')$ shown in Figure 9. It is slightly broader than the usual single-level RRKM translational energy distribution calculated by assuming all the molecules dissociate from the level 16.64 kcal/mol above the dissociation limit. Acceptable fits to the TOF data could also be obtained with an "averaged" 22.61-kcal/mol $P(E')$ and an averaged 10.68-kcal/mol $P(E')$, but not from dissociating levels peaked at higher or lower energies than these. Thus the measured C_2H_5O TOF suggests that most of the detected radical products were formed from DEE dissociating from the energy levels between 5 and 28 kcal/mol above the 81.8-kcal/mol dissociation limit (including energy levels in the population distribution weighted by a factor of 60 or greater). It should be noted that since the excited diethyl ether molecule is travelling ~ 1120 m/s through a small region (~ 3 mm long) viewed by the detector, we are only sensitive to molecules with dissociation times less than a few microseconds. When the calculated RRKM dissociation rate constant of 0.5641×10^4 s⁻¹ is used, one finds that only about 1% of the DEE that dissociates to radical products at 16.64 kcal/mol above the dissociation limit will dissociate within the detector viewing volume and have a chance to be detected.

2. $C_2H_2OC_2H_5 \rightarrow C_2H_5OH + C_2H_4$. The fast peak in the m/e 31 TOF (Figure 2) was fit with a completely flexible point form for the $P(E')$. The dotted curve fit to the TOF spectrum shown in Figure 2 was calculated from the $P(E')$ shown in Figure 11. This $P(E')$ peaks near 26 kcal/mol and extends out to beyond 45 kcal/mol, with an average energy released of ~ 24 kcal/mol. The curves fit to the fast peaks in the m/e 26 and 27 TOF's (Figures 8 and 7) were calculated from this $P(E')$ by using the relative contribution of the C_2H_5OH and C_2H_4 to these masses as the only variable parameter.

Assuming (1) the A factor and activation energy of István and Péter for this channel are correct and (2) the conclusions about the energy levels these molecules which

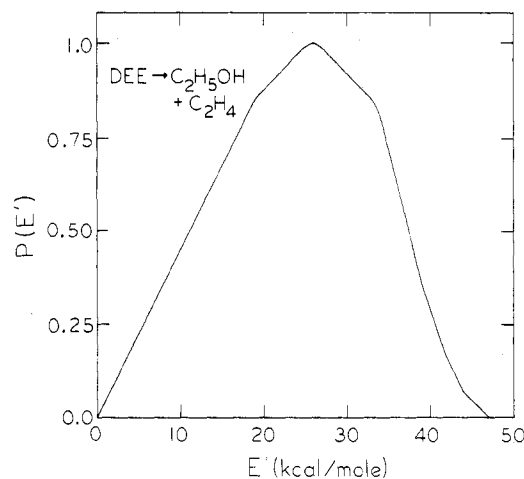


Figure 11. Center-of-mass translational energy distribution for the molecular elimination channel $DEE \rightarrow C_2H_5OH + C_2H_4$ derived from the ethanol contribution to the m/e 31 TOF distribution (Figure 2). This $P(E')$ was used to obtain the calculated fits shown in all other TOF distributions which contained contributions from C_2H_5OH or C_2H_4 .

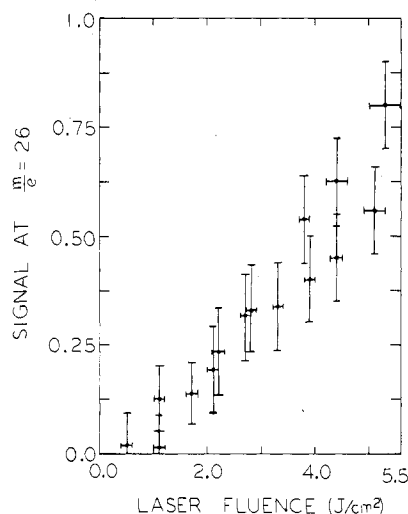


Figure 12. Integrated signal at m/e 26 as a function of photon energy fluence: (●) experimental points. Error bars represent plus or minus one standard deviation of the statistical counting error. The laser pulse shape is constant, so the intensity increased with fluence.

dissociated to radicals had reached are also correct, we can estimate the energy levels from which the molecules dissociated to ethanol and ethylene. Since the RRKM rate constants for the molecular elimination channel are higher than those for the radical channel for internal energies up to ~ 125 kcal/mol (see Figure 12), molecular eliminations will occur on the average from slightly lower energy levels. How much lower will depend on the mean energy level from which the radical dissociations occur and the fraction of molecules that dissociate during the laser pulse. A good estimate based on our approximate modeling is that the molecules that dissociate via reaction 2 and are detected do so from energy levels that are 1–9 kcal/mol below the energy levels from which the radical products are formed. We thus estimate that the DEE dissociates to give molecular products from energy levels mostly between 82 and 107 kcal/mol above its zero point level. This energy range is compared to that of the DEE that dissociates to radical products from a group of energy levels mostly between 87 and 110 kcal/mol above its zero point level.

D. Branching Ratio and Total Product Yield Dependence on Laser Power. The integrated TOF signal at m/e 26 as a function of laser power is shown in Figure 12. In

(16) Or if all these levels are not above the dissociation limit, as for the case when 10.68 kcal above the dissociation limit, we used a narrower distribution: 8, 20, 60, 80, 60, 20, 8.

spite of the large error bars, one can see the signal still increased with laser power at the higher powers used in this experiment. Quantitative interpretation of this data is, however, quite difficult in this case. There are two dominant factors which would cause our signal level to rise in this measurement. The first is simply that more molecules absorb enough photons during the laser pulse to reach energy levels above one or both dissociation limits. The second factor arises from our experimental arrangement. An excited DEE molecule will spend at most 2.7 μ s in the viewing region of the detector. Because the lifetimes for dissociation to molecular or radical products at an energy level of 98 kcal/mol above the ground state are \sim 13 and \sim 180 μ s, respectively, we detect only a small fraction of the total number of dissociations. With increasing laser power, the average energy level a molecule will reach above the dissociation limit increases. At the higher excitation levels, the dissociation rate constants become higher and a greater fraction of the molecules will dissociate within the region viewed by the detector. Even when most of the molecules are already above the dissociation limit and no increase in the number of molecules above the dissociation limit is expected, higher laser intensity will still give a larger signal. For instance, the fraction of dissociations forming radical products that occur within the viewing region of the detector increases by a factor of 3, from \sim 1 to \sim 3%, if the molecules dissociate from an energy level 19.63 kcal/mol compared to 16.64 kcal/mol above the dissociation limit.

A crude determination of a branching ratio between these two channels was made by comparing the total signal at m/e 14, 15, 26, 27, 28, and 29 ascribed to C_2H_5 with the total signal at all the masses counted ascribed to C_2H_5OH . If the branching ratio were 1:1, and the ionization cross sections are the same we would expect the total ion signal from C_2H_5 to be 10.8 times that of C_2H_5OH due to the differences in laboratory angular and velocity distribution of these two products. The observed total ion signal for C_2H_5 is 3.0 times that for C_2H_5OH , giving a branching ratio of 78% molecular channel and 22% radical channel. The analysis of the total ion signals of C_2H_5 compared to C_2H_4 gives a similar branching ratio. However, the percent ion signal of C_2H_5O compared to C_2H_5OH gives a branching ratio of 95:5. Our lack of data at m/e 45 may be the source of the discrepancy, but as this would only shift the branching ratio in favor of the molecular channel in the comparison of the C_2H_5 and C_2H_5OH counts and would not affect the C_2H_4 : C_2H_5 ratio, we may arrive at a lower bound of \sim 70% molecular channel. The branching ratio predicted from the rate parameters is critically dependent on the mean energy level from which the molecules dissociate for each channel. In a calculation where the molecular products are formed from energies peaked at 107 kcal/mol above the ground state of DEE and the radical products are formed from 3 kcal/mol higher energies, the branching ratio is 85.3 and 14.7% in qualitative agreement with our crude estimate.¹⁷ Our best estimate of the energy levels from which dissociation occurred, based on the translational energy distribution obtained from the m/e 44 TOF, was \sim 9 kcal/mol lower; at these lower energies

the radical channel would be $<$ 5% of the dissociation yield.

IV. Discussion

The effect that an exit channel barrier has on the asymptotic translational energy distribution of the products has been treated theoretically by Marcus¹⁸ and Hase et al.¹⁹ Hase et al.¹⁹ studied ethyl radical decomposition to $H + C_2H_4$ with Monte Carlo classical trajectories on potential energy surfaces with different exit channel barrier heights. The exit channel barrier results from the C-C single bond in the reactant shortening to a C=C double bond in the ethylene product. He found that the shape of the product translational energy distribution at the top of the barrier agreed with the predictions of RRKM theory, but that the distribution broadened and shifted to higher translational energies as the reaction was allowed to proceed beyond the top of the exit channel barrier. The effect was larger for a 3.5-kcal/mol barrier than it was for a 0.1-kcal/mol barrier. Marcus¹⁸ demonstrated the application of RRKM theory to prediction of final product translational energy distributions when the reaction proceeds through a tight transition complex which involves an exit channel barrier. He showed that one should allow for the evolution of the RRKM transition state as the reaction proceeds down the exit channel barrier. In this example case, the bending vibrations excited in the tight transition state are coupled into translation and rotation of the products as they recoil from each other.

The concerted reaction forming ethanol and ethylene has a large exit barrier estimated at \sim 50 kcal/mol. The measured product translational energy distribution shown in Figure 11 peaks at \sim 24-kcal/mol translational energy. At an RRKM critical configuration calculated from the István and Péter A factor and activation energy only 1.5–2.5 kcal/mol is in the relative motion of the products, if the molecule dissociates from energies averaging around 14, and 39 kcal/mol, respectively, above the dissociation limit, so one might conclude that the interactions between the products as they descend the exit barrier considerably alters their energy distribution at the top of the barrier. Their final translational energy is measured to be almost 1/2 of the exit barrier height.

The fraction of the exit channel barrier energy released to translation in this four-center elimination reaction is significantly higher than that measured for the four-center HCl elimination from halogenated hydrocarbons by Sudbo et al.,³ but considerably smaller than the 70% released to translation in the IRMPD dissociation of ethyl vinyl ether to $CH_3CHO + C_2H_4$.² The latter comparison is particularly interesting as both involve hydrogen atom transfer and breaking of a C-O bond, as here both bonding electrons move away from the CO bond in a concerted reaction, the C-O interaction becomes repulsive, and the translational energy of the product molecules is mainly due to the repulsive energy release of this interaction. Although the fractions of the exit barriers appearing in translational energy are somewhat different for EVE and DEE, they have a similar average translational energy release, 31 and 26 kcal/mol, respectively. In concerted reactions with large exit barriers, the structure of the transition state will determine the energy partitioning to a large extent. If the chemical bonds in the products which are to be formed are extensively stretched in the transition state, significant vibrational excitation is expected. On the other hand, the longer the bond which is to be broken is extended, the less

(17) For this calculation, the spread of energy levels from which dissociation in the viewing region of our detector occurred was comparable to that described in part 3C. We used a ground-state photon absorption cross section of 1×10^{-18} cm² which fell exponentially to 3.2×10^{-19} at the radical dissociation limit. The excitation level described was reached at a photon fluence of 1.83 J/cm²; this was the average excitation of the molecules that dissociated in the collision region. The average excitation of all the molecules at the end of the laser pulse was \sim 80 kcal/mol. These parameters predicted a larger increase in signal with increasing laser power than our data showed.

(18) R. A. Marcus, *J. Chem. Phys.*, **62**, 1371 (1975).

(19) W. L. Hase, R. J. Wolf, and C. S. Sloane, *J. Chem. Phys.*, **71**, 1911 (1979).

important the repulsive energy release will be. In the four-center HCl elimination reactions, the C-Cl bond to be broken must be significantly extended, but in EVE or DEE, in view of the enormous translational energy release it is likely that the C-O bonds to be broken are not significantly extended when the interaction suddenly becomes repulsive.

The shape of the product translational energy distribution (Figure 9) for radical channel 1 was in agreement with RRKM theory for reactions proceeding through a loose transition state. We accounted for the fact that, in an IRMPD experiment, the reactant molecules dissociate from a distribution of energy levels above the dissociation limit by using an averaged RRKM $P(E')$ to fit the data. The exact form of this distribution was described in part IIIC. The best fit $P(E')$ was calculated with molecules dissociating to radicals from a spread of energy levels peaked at 16.64 kcal/mol above the dissociation limit. The average energy released to translation of the radical products detected was 1.6 kcal/mol.

Because the photon absorption and stimulated emission cross sections as a function of energy for a highly energized

molecule are not generally known, one is usually uncertain in an IRMPD experiment as to what mean energy level the absorbing molecule will reach before it dissociates. An attempt was made in this study to reduce this uncertainty considerably. Assuming (1) that the thermochemical A factor and activation energy reported for the dissociation channel are correct and (2) that the translational energy distribution of the products is correctly predicted by RRKM theory, one can determine the approximate mean energy level from which the molecules dissociated to radicals by attempting to fit the data with various predicted RRKM $P(E')$'s. The mean total available energy for the RRKM $P(E')$ that fit the measured velocity distribution determines the mean energy level from which the molecules dissociated. The method is only weakly dependent on the assumed shape of the distribution of energies of the dissociating levels.

Acknowledgment. This work was supported by the Office of Naval Research under Contract N00014-75-C-0671.

Registry No. Diethyl ether, 60-29-7.

Study of Isotope Effects in Benzene Dimers in a Seeded Supersonic Jet

K. H. Fung, H. L. Selzle,* and E. W. Schlag

*Institut für Physikalische und Theoretische Chemie, Technische Universität München, D 8046 Garching, West Germany
(Received: June 14, 1982; In Final Form: June 20, 1983)*

Mixtures of isotopically labeled species expanded in a hypersonic jet lead to a complex mixture of dimer spectra which can be disentangled by measuring the excitation spectrum in coincidence with a multiphoton mass spectrum. The spectra reveal that the electronic excitation is substantially localized in one or the other of the benzene rings. The spectrum reveals a clear splitting of the dimer for which general possible explanations are discussed. Multiphoton ionization here permits the selective identification of each of the three isotopically mixed absorption spectra; such mixed spectra give new information about molecular interactions.

Introduction

The techniques of two-color mass-selective resonance-enhanced photoionization together with a supersonic jet has been shown to be a very effective way of studying clusters in the gas phase.^{1,2}

Supersonic jets have been widely used to obtain spectra of isolated ultra cold molecules in the gas phase that are free of thermal congestion.³ It is also known that during the isentropic expansion aggregation can occur and produce van der Waals complexes and clusters.⁴ Typically many such possible clusters are formed simultaneously, their identification being usually derived from their pressure dependence.⁵ A direct identification of these

complexes becomes indispensable if one is to follow their strongly overlapping spectra individually. Mass spectroscopic identification appears here as the method of choice; however, the fragile nature of these van der Waals complexes makes it necessary to employ extreme soft ionization techniques. Electron impact leads to massive fragmentation and is not species specific. Multiphoton ionization appears as the method of choice, since it can directly identify the mass of the species associated with any particular absorption wavelength. Here the first photon is tuned to the transition of interest, the second photon being added to this to produce the corresponding ions. Two photons often suffice for ionization. This method often fails for van der Waals molecules since in single-color experiments the second photon often greatly exceeds the ionization potential, leading to dissociation of the van der Waals ions.

To achieve soft ionization of the intact van der Waals ions one needs to reduce the energy of the second step until ionization is just matched, hence a second color must be

(1) K. H. Fung, W. E. Henke, T. R. Hays, H. L. Selzle, and E. W. Schlag, *J. Phys. Chem.*, **85**, 3560 (1981).

(2) J. B. Hopkins, D. E. Powers, and R. E. Smalley, *J. Phys. Chem.*, **85**, 3739 (1981).

(3) R. E. Smalley, L. Wharton, and D. H. Levy, *Acc. Chem. Res.*, **10**, 139 (1977).

(4) S. Leutwyler, U. Even, and J. Jortner, *Chem. Phys. Lett.*, **86**, 439 (1982); A. M. Griffiths and P. A. Freedman, *ibid.*, **63**, 469 (1981); D. V. Brumbaugh, C. A. Haynam, and D. H. Levy, *J. Chem. Phys.*, **73**, 5380 (1980); T. R. Dyke, K. M. Mack, and J. S. Muenter, *ibid.*, **66**, 498 (1977); K. C. Janda, J. C. Hemminger, J. S. Winn, S. E. Novick, S. J. Harris, and W. Klemperer, *ibid.*, **63**, 1419 (1975).

(5) A. Amirav, U. Even, and J. Jortner, *J. Chem. Phys.*, **75**, 2489 (1981), and references therein; R. E. Smalley, L. Wharton, and D. H. Levy, *ibid.*, **66**, 2750 (1977).